VOL. 18, NO. 4, FEBRUARY 2023 ISSN 1819-6608
ARPN Journal of Engineering and Applied Sciences

www.arpnjournals.com

PALMPRINT AUTHENTICATION USING SYMBOLIC AGGREGATE APPROXIMATION FEATURES WITH IMPROVED ENHANCEMENT TECHNIQUES

S. Palanikumar[1], M. P. Flower Queen[2], S. Mathupriya[3] and K. Tharageswari[4]
[1]Department of Computer Science and Business System, Vel Tech Multi Tech Dr. Rangarajan Dr. Sakunthala Engineering College, Avadi, Chennai, Tamil Nadu, India
[2]Department of Electrical and Electronics Engineering, SRM TRP Engineering College, Trichy, Tamil Nadu, India
[3]Department of Computer Science and Engineering, Sri Sairam Institute of Technology, Chennai, Tamil Nadu, India
[4]Department of Computer Science and Engineering, Faculty of Engineering, Karpagam Academy of Higher Education, Coimbatore, Tamil Nadu, India
E-Mail: tharahari1515@gmail.com

ABSTRACT

The palmprint enhancement is a pre-processing stage of palmprint authentication. The accuracy of the recognition rate can be improved by incorporating effective palmprint enhancement methods. So far, only a little work has been done in palmprint enhancement. Little attention is given to incorporate the enhancement techniques in palmprint authentication system to achieve performance improvement. This work presents robust enhancement methods which provide better performance and accuracy. Palmprint enhancement using curvelet and Recursive Histogram Equalization (RHE) overcomes the drawbacks of the existing systems and makes palmprint recognition simpler and more accurate with enhanced palm image as input. Palmprint recognition system uses the Symbolic Aggregate Approximation (SAX) features from the enhanced palmprint image. The recognition rate is optimum when both curvelet and RHE methods are used for enhancement of palmprint. Here we compared different types of enhancement methods and we have obtained maximum recognition rate with a combination of recursive histogram equalization and curvelet transform. The performance of the palmprint authentication is measured by False Acceptance Rate (FAR), False Rejection Rate (FRR) and Total Success Rate (TSR). The comparison of recognition rate with enhancement is done using minimum distance classifier, Support Vector Machine, Random Forest and Bayesian. Random Forest classifier provides better results.

Keywords: palmprint authentication, symbolic aggregate approximation features, improved enhancement techniques.

1. INTRODUCTION

There exist three different categories for palmprint authentication, divided on the basis of extracted features; (i) line-based approaches. (ii) appearance-based approaches [1] and (iii) texture-based approaches [2]. Line-based methods [3] are based on line matching, line detection, crease detection, morphological operators etc. Morphological operators [4] can be used in the feature extraction process in order to obtain the feature vectors. Datum point invariant and the line feature matching technique for the verification process are not appropriate for many online security systems, since it is difficult to extract principal lines from a low-resolution palmprint image [5]. The required recognition rates and computational efficiency are not fully achieved here. Other issues in the line-based approaches include the existence of similar line features in many palmprints, and the thickness and width of the different lines are not taken into account which is very critical for differentiating palmprints [6].

Appearance-based approaches are based on the analysis of principal component and linear discriminate. The original training palmprints are transformed into small groups of characteristic feature images called eigen palms [1] by means of Karhunen-Loeve (K-L) transform. But the authentication performance of these eigenpalms is reduced when it is applied in real time applications.

In texture-based approach, texture features are extracted by means of gabor filter, discrete cosine transform, ordinal filter, laws mask, discrete fourier transform, wavelets and so on. Even though the Gabor filter [7], [8] gives accurate time-frequency location and robustness against varying image's brightness and contrast, it involves high computational cost and time delay. Difficulty in setting an appropriate filter parameter causes identification performance to depend much on the training set used for parameter selection. Orthogonal line ordinal feature [5] is currently the best ordinal measure for palmprint representation; still its theoretical foundation has not been well formulated. Wavelet Energy Feature technique's ability to distinguish palms is very strong because it can reflect the wavelet energy distribution of the principal lines, wrinkles and ridges in different directions at varying wavelet decomposition levels. Disadvantages of this method are its sensitiveness towards noise, the requirement of high-resolution images, implementation cost and time complexity. Fourier transform method is used to ignore the abundant textural details of a palm, and the extracted features are highly influenced by the lighting situations. A huge storage of database to store image templates affects the system's simplicity.

Personal verification using palmprint and hand geometry biometric [9] does verification by integrating hand geometry features. Palmprint and hand geometry features are acquired using a digital camera. These images are aligned and then used to extract palmprint and hand geometry features. These features are then examined for their individual and combined performances. The image

acquisition setup used in this work is inherently simple and it does not employ any special illumination, nor does it use any pegs to cause any inconvenience to the users.

Hierarchical palmprint identification via multiple feature extraction [10] describes a new method to authenticate individuals based on palmprint identification and verification. A texture-based dynamic selection scheme is used to facilitate the fast search for the best matching of the sample in the database in a hierarchical fashion [11]. The global texture energy, which is characterized with high convergence of inner-palm similarities and good dispersion of inter-palm discrimination, is used to guide the dynamic selection of a small set of similar candidates from the database at coarse level for further processing. Multiple palmprint features are used by Nanni and Lumini for accurate palmprint recognition.

Combining multiple classifiers by averaging or by multiplying [12], [6] combines observations from different sources. Palmprint-based recognition system using phase difference information [13] used histogram equalization for enhancing the contrast of the palmprint image. Tamrakar and Khanna [14] applied block wise Gaussian derivative phase pattern histogram for palmprint recognition. Li and Zhang [15] presented a technique for palmprint identification based on Quantum algorithm. Most of the works did not give any attempt to incorporate the enhancement techniques in biometric palmprint images to achieve performance improvement. In most of the prior systems, the enhancement stage got little attention. The enhancement of the input image can deeply affect the output of the system. This work incorporates curvelet and RHE techniques for enhancement of the palmprint image [16]. Curvelet is used for removing noise in the palmprint image, and RHE is used for improving the contrast of the palmprint image. Applying curvelet and RHE improves the overall performance of the system. Table 1 highlights the state of art work done in the field of palm print recognition using different types of feature extraction method and classification.

1.1 Palmprint Enhancement Techniques

Enhancement of the palm print images before feature extraction and classification improves the recognition rate.

Table-1. Comparative of various methods in literature for palm print recognition.

Methods adopted	Features Extracted	Recognition /Accuracy (%)	Reference Number
Statistical Methods - PCA LDA ICA Stockwell DCT Fisherface Gabor filter Zernike moment	Eigen palm	99.1	[20]
	ICA basis	98.67	[21]
	Fishers Linear Discriminant	99	[22]
	Instantaneous phase difference using Stockwell transform	>99	[23]
	DCT + Fisherface method	98.13	[24]
	2-d Gabor phase encoding	97(GAR)	[25]
	Fusion code from multiple elliptical Gabor filter	96.3(GAR)	[26]
	Competitive Coding Scheme and angular matching	98.4%(GAR)	[27]
	Orthogonal line ordinal	0.2(EER)	[28]
	Wavelet based feature	99 (GAR)	[29]

Different types of [17] enhancement methods are explored namely Histogram Equalization (HE), Weighted Threshold Histogram Equalization method (WTHE), [18] Adaptively Increasing Value of Histogram Equalization method (AIVHE), Bin Underflow and Bin overflow (BUBO), Histogram modification method, Recursive Histogram Equalization, Curvelet transform, Genetic algorithm based enhancement. Effectiveness of the enhancement algorithm is measured by means of absolute mean brightness error (AMBE), entropy and peak signal to noise ratio (PSNR). The effectiveness of the different enhancement algorithm for palmprint image enhancement is discussed in [19]. Table-2 shows the computation complexity of different enhancement methods. In terms of accuracy and processing time. Recursive Histogram Equalization method and Curvelet transform based enhancement method gives the optimized result. Hence, in the proposed scheme, RHE & Curvelet based enhancement is applied before feature extraction.

1.2 Conventional Histogram Equalization

The traditional histogram equalization technique is described as follows:

Consider the input image as X. Based on the histogram H(X), the Probability Density Function (PDF) of the image is defined as

$$p(k) = n_k/N = n_k/ (n_0+n_1+\ldots+n_{L-1}) \text{ for } k = 0,1,\ldots.L-1 \quad (1)$$

where n_k is the number of pixels that have the gray level k appears on the input image X and N is the total number of pixels in the input image. Note that $p(k)$ is associated with the histogram of the input image which represents the number of pixels that have a specific intensity X_k. The graphical appearance of PDF is known as the histogram.

From the PDF in equation (1), the cumulative distribution function (CDF) is defined as

$$c(k)=\sum_{j=o}^{k} p(j) \quad \text{for k=0,1….L-1} \tag{2}$$

Note that $c(L-1) = 1$ from equations (1) and (2).

Based on the CDF, histogram equalization now maps an input gray level $X_k$into an output gray level $f(k)$, where $f(k)$ which is commonly called as *level* transformation function, is defined as

$$f(k)= X_0 + (X_{L-1} - X_0) \, . \, c(k) \tag{3}$$

where X_0 is the minimum gray level and X_L is the maximum gray level. Thus, histogram equalization remaps the input image into the entire dynamic range $[X_0, X_{L-1}]$.

1.3 Bin Underflow and Bin Overflow

A global HE-based enhancement method that uses the BUBO mechanism is proposed. The PDF of the image is thresholded using a lower (underflow) threshold and an upper (overflow) threshold, where CBU and CBO are bin underflow and bin overflow thresholds. HE is performed using the thresholded histogram. BUBO is an effective technique for contrast enhancement but in some cases the method still can not expand gray level distribution to expand dynamic range of input image. Although we can add the function of adjusting parameter into BUBO to expand image for more dynamic range and the method still need to adjust different parameter for input images. To overcome the drawbacks of the Traditional HE Methods, the BUBO method puts constraint to avoid over enhancement by,

$$P_{BUBO}(k) = \begin{cases} C_{BO}, & if \quad P(k) > C_{BO} \\ P(k), & if \quad C_{BU} \le P(k) \le C_{BO} \\ C_{BU}, & if \quad P(k) < C_{BU} \end{cases} \tag{4}$$

$C_{BU} = (1- \alpha)/N$

$C_{BO} = (1+ \alpha)/N$

Where α varies from 0 to infinity, and N is the total number of pixels in the given input image. It cannot expand grey-level distribution to expand dynamic range of input image. To expand image for more dynamic range the method still need and adjust different parameter for input images.

1.4 Weighted Threshold Histogram Equalization

The WTHE enhancement method performs histogram equalization based on a modified histogram. Each original probability density value $p(k)$ in equation (1) is replaced by a weighted and thresholded PDF value $p_{wt}(k)$ yielding

$$\Delta k = (L-1) \times p_{wt}(k) \tag{5}$$

$p_{wt}(k)$ is obtained by applying a transformation function TR(k) to p(k), that is,

$p_{wt}(k) = TR(p(k))$

$$TR(p(k))= \begin{cases} p_u & if \quad p(k) > p_u \\ \left[\dfrac{p(k)-p_l}{p_u-p_l} \right]^r \times p_u & if \quad p_l \le p(k) \le p_u \\ 0 & if \quad p(k) < p_l \end{cases} \tag{6}$$

The original PDF is clamped at an upper threshold p_u and a lower threshold p_l and transforms all values between the upper and lower thresholds using a normalized power law function with index $r>0$. The increment for each intensity level is decided by the transformed histogram. The increment can be controlled by adjusting the index r of the power law transformation function. To give an example, when $r<1$, the power law function will give a higher weight to the low probabilities in the PDF than the high probabilities. Therefore, with $r<1$, the less-probable levels are "protected" and over-enhancement is less likely to occur. Besides the weighting mechanism described above, the PDF is also thresholded at an upper limit p_u. As a result, all levels whose PDF values are higher than $p_u$will have their increment clamped at a maximum value $\Delta_{max}=(L-1)p_u$. Such upper clamping further avoids the dominance of the levels with high probabilities when allocating the output dynamic range. In our algorithm, the value of $p_u$is decided by

$$p_u = v \, . \, P_{max}, 0 < v \le 1 \tag{7}$$

where $Pmax$ is the peak value (highest probability) of the original PDF and the real number v defines the upper threshold normalized to $Pmax$. It can be seen from the equation (6), that when r=1, p_u=1 and p_l=0 the WTHE method reduces to the original HE. Some other global HE-base methods, such as the BUBO method, can also be considered special cases of the WTHE method. Our experiments show that for a large variety of images, the value of v can be kept constant while achieving satisfactory effect of enhancement. After obtaining the weighted thresholded PDF $p_{wt}(k)$, the equalization process is similar to the traditional HE. The cumulative distribution function (CDF) is first obtained by

$$C_{wt}(k)=\sum_{m=0}^{k} p_{wt}(m), \text{ for } k=0,1,\ldots..L-1 \tag{8}$$

and HE procedure is then performed as

$$G(i,j)=W_{out} \times C_{wt}(F(i,j)) + M_{adj} \tag{9}$$

where W_{out} is the dynamic range of the output image. M_{adj} is the mean adjustment factor that compensates for the mean change after enhancement. For a simple case, W_{out} is equal to the full range [0, L-1], and M_{adj}=0. W_{out}= min(L-1,G_{max}.W_{in}) in which $W_{in}$is the dynamic range of the input image and G_{max} is a pre-set maximum gain of dynamic range. We usually set G_{max} in the range of 1.5 to 3.0.

1.5 AIVHE Contrast Enhancement Method

The method reshapes the original PDF to obtain new PDF to prevent a significant change in the gray levels. It also provides a mechanism of adjustment to contrast enhancement by means of adaptive constraint parameter $\alpha(k)$ for adjustment automatically, which is determined by the initial value γ and user defined-parameter β. AIVHE divides the original PDF into upper and lower blocks on the basis of P_{bas}. A value of maximum threshold P_h is then be set to restrict the variation of the *PAIVHE (k)*, and then limit the value of *PAIVHE (k)* be not greater than P_h. AIVHE reshapes original PDF and obtain the *PAIVHE (k)* by,

$$P_{AIVHE}(k) = \begin{cases} P_h, & if \quad P(k) \geq P_h \\ P(k) - \alpha(k)(P(k) - P_{bas}) \times \beta, & if \quad P_{bas} < P(k) < P_h \\ P(k) + \alpha(k)(P_{bas} - P(k)) \times \beta, & if \quad P(k) \leq P_{bas} \end{cases} \quad (10)$$

where P_{bas} is set to the average PDF, P_h is set as double of P_{bas}, β is the enhancement parameter adjusted by user, and $\alpha(k)$ is adaptive constraint parameter for adjustment automatically. The initial value for β is a real number in the range of [0, 1]. The function of HE is produced when β is set to zero and P_{bas} is the mean value of the maximum and minimum value of *P(k)*. Dark and bright regions stretching are controlled by γ at $\alpha(k)$. Whole contrast enhancement effect of the image is controlled by β. The effective constraint parameter can be calculated as

$$\alpha(k) = \begin{cases} (1-(X_m-k)/X_m)^2 \times (1-\gamma) + \gamma & if, \quad k \leq X_m \\ (1-(k-X_m)/((L-1)-X_m))^2 \times (1-\gamma) + \gamma & if, \quad k > X_m \end{cases} \quad (11)$$

where, $X_m$is the mean brightness, γ is the real number and the initial value in the range of [0, 1]. It decides the distribution of pixels in dark and bright region. By the $P_{AIVHE}(k)$, the cumulative distributive function, $C_{AIVHE}(k)$ is found. $C_{AIVHE}(k)$ is normalized and then the output image is as follows,

$$f(k) = (L-1) \times (C_{AIVHE}(k))/(C_{AIVHE}(k)(L-1)) \quad (12)$$

where $f(k)$ is the input/output transfer function, L-1 is the maximum gray level, k is the k^{th}gray level, $C_{AIVHE}(k)$ is the cumulative density function .Furthermore, AIVHE method enhances the contrast but the brightness of the palmprint is not preserved.

1.6 Brightness Preserving Bi-Histogram Equalization

The BBHE firstly decomposes an input image into two sub-images based on the mean of the input image. One of the sub-images is the set of samples less than or equal to the mean whereas the other one is the set of samples greater than the mean. Then the BBHE equalizes the sub-images independently based on their respective histograms with the constraint that the samples in the formal set are mapped into the range from the minimum gray level to the input mean and the samples in the latter set are mapped into the range from the mean to the maximum gray level.

Denoted by $X_{m,}$ the mean of the image X and assume that $X_m \in \{X_0, X_1, ..., X_{L-1}\}$. Based on the mean, the input image is decomposed into two sub images $X_L$and $X_U$as

$$X = X_L \cup X_U \quad (13)$$

Where, $X_L = \{X(i,j) \mid X(i,j) \leq X_m, \forall X(i,j) \in X\}$
And
$X_U = \{X(i,j) \mid X(i,j) > X_m, \forall X(i,j) \in X\}$
Note that the subimage$X_L$is composed of $\{X_0, X_1, ,. . . , X_m\}$ and the other sub image $X_U$is composed of $\{X_{m+1}, X_{m+2}, . . . , X_{L-1}\}$.

Table-2. Comparison of computation time for different enhancement techniques.

Enhancement method	Computation time(sec)
Histogram Equalization	0.1018
Bin underflow Bin overflow	0.1063
Weighed threshold histogram equalization method	0.1137
Adaptively increasing value of histogram equalization method (AIVHE)	0.1382
Recursive Histogram equalization(RHE)	0.2074
Bi histogram equalization with threshold	0.1859

2. PALMPRINT RECOGNITION USING SAX FEATURES

The symbolic demonstration of time series is called SAX. It transforms the original time-series data into symbolic strings where Piecewise Aggregate Approximation (PAA)-based algorithm is used that provides simplicity and low computational complexity. Since SAX requires less storage space, it is used for solving many challenges associated with the present data mining tasks. In addition, the symbolic representation allows researchers seek further to the available wealth of data structures and string manipulation algorithms in computer science, and also for many applications in bioinformatics and data mining [30] [11].

SAX algorithm transforms a time-series X of length ‘n’ into the string of arbitrary length w, where w <

n, using a table that contains the breakpoints. Each value in the table corresponds to each level in the time series graph which is further represented by symbols in the alphabet array of size>2 which finally forms the string of length 'w'. Dimensionality reduction is based on two parameters named 'sax length' (w) and 'number of symbols used in the alphabet array'. The algorithm consists of two steps. In the first step, it transforms the original time-series into a PAA representation ($\overline{C}$) and this intermediate representation is further converted into alphabetic string ($\hat{C}$) in the second step. Usage of PAA approach in the first step gives the advantage of being simple and efficient in dimensionality reduction and provides lower bounding property. The second step, where the actual conversion of PAA coefficients into alphabets is also computationally efficient, shows the contractive property of symbolic distance.

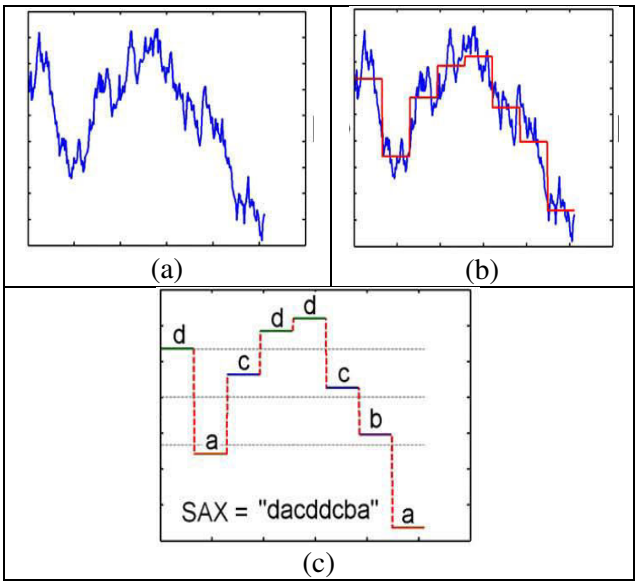

Figure-1. Times series to SAX representation (a) Time series, (b) PAA representation, (c) SAX representation.

Generating SAX from PAA representation of a time series is implemented in a way which produces symbols that correspond to the varying magnitude of time-series data. Figure-1 shows the conversion of times series into SAX representation. Figure-1 (a) is the original time series data. Figure-1 (b) shows the corresponding PAA representation and Figure-1(c) shows the SAX representation.

3. DIGITAL CURVELET TRANSFORM

A transform for digital n by n data is analogous to the discrete curvelet transform of a continuous function $f(x_1, x_2)$. Each of the continuum concepts is replaced with the appropriate digital concept. In general, the translation is rather obvious and direct. It is found that rather than merging the two dyadic subbands $[2^{2s},2^{2s+2}]$ and $[2^{2s+1},2^{2s+2}]$ as in the theoretical work, in the digital application, leaving these subbands separate, applying spatial partitioning to each subband and applying the ridgelet transform on each subband separately leads to improved visual and numerical results. The à troussubband filtering algorithm is especially well-adapted to the needs of the digital curvelet transform. The algorithm decomposes an $n \times n$ image as a superposition of the form as given in Equation (14)

$$I(x,y) = c_J(x,y) + \sum_{j=1}^{J} w_j(x,y) \quad (14)$$

where c_J is a coarse or smooth version of the original image I, and w_j represents the details of I at scale 2^{-j}. Thus, the algorithm outputs J + 1subband arrays of size $n \times n$. Here, j = 1 corresponds to the finest scale (high frequencies).

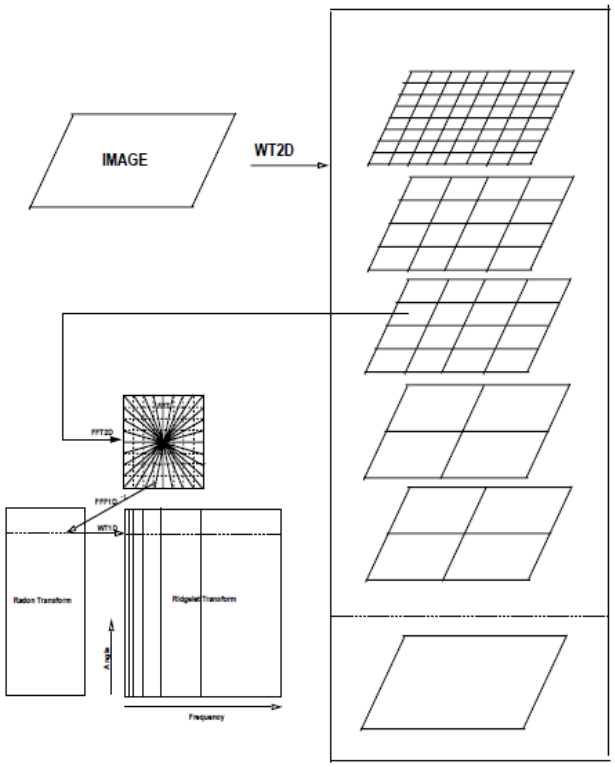

Figure-2. 14 Block diagram of the curvelet transform.

Figure-2 shows the block diagram of the curvelet transform. First the original image is decomposed into subbands. Then spatial partition for each subband is done. Finally, the ridgelet transform is applied to each block.

Discrete curvelet transform algorithm is given below.

Step1 : Apply the à trous algorithm with *J* scales
Step2 : Set $B_1 = B_{min}$
Step3 : For j = 1,….*J* do

Partition the subband w_j with a block size B_j and apply the digital ridgelet transform to each block
If j modulo 2 =1 then $B_{j+1}=2\ B_j$
Else $B_{j+1}= B_j$

The side length of the localizing windows is doubled at every otherdyadic subband, thus maintaining the fundamental property of the curvelet transform which says that the elements of length about $2^{-j/2}$ serve for the analysis and synthesis of the j^{th}subband $[2^j, 2^{j+1}]$.

The noisy image is represented as in Equation (15)

$$x_{i,j} = f(i, j) + \sigma z_{i,j} \quad (15)$$

where f is the image to be recovered and z is the white noise.

Hard thresholding can be used for denoising as given in Equation (16) and Equation (17)

$$\hat{y}_\lambda = y_\lambda \quad \text{if} \quad |y_\lambda| / \sigma \geq k\hat{\sigma}_\lambda \quad (16)$$

$$\hat{y}_\lambda = 0 \quad \text{if} \quad |y_\lambda| / \sigma < k\hat{\sigma}_\lambda \quad (17)$$

where y_λ is the noisy curvelet coefficient. k value is 4 for first scale and $k = 3$ for others.

Soft thresholding is efficient and more sophisticated than hard thresholding. In this work, soft thresholding given by Patil and Singhai (2010) is used. The same technique is used for wavelet and contourlet denoising.

The curvelet-based denoising algorithm is given below.

Step1 : Apply two dimensional discrete curvelet transform to noisy image.

Step2 : Estimate the subband dependent BayesShrink threshold.

Step3 : Threshold the curvelet coefficients by applying soft thresholding technique. Curvelet has more orientations with right frame. Curvelet transform has scale, translation and orientations. So curvelet coefficients are expressed in cell.

Step4 : Perform two dimensional inverse discrete curvelet transform and reconstruct the denoised image.

One of the most popular supervised learning deep learning approaches, the support vector machine, is used for both classification and regression problems. However, it is mostly used in machine learning to address categorisation problems. The SVM algorithm's goal is to identify the ideal set point or line that can categorize n-dimensional space, enabling us to rapidly classify new data points in the hereafter. This best decision boundary is known as a hyperplane. SVM chooses the maximum vectors and points to help build the hyperplane. Due to these severe circumstances, also known as qs support vectors; the method is referred to as a Support Vector Machine.

4. ADVANCED PALMPRINT RECOGNITION SYSTEM

The proposed palmprint recognition system using SAX features is shown in Figure-3. It composes input acquisition, enhancement, feature extraction and recognition stages. The input acquisition and enhancement steps are discussed in chapter I, II, and III. This chapter mainly focuses on the feature extraction and recognition steps. The block diagram of palmprint recognition using SAX features is shown in Figure-3.

Here, an extension of the SAX is used which represents the 2D data using a 2D matrix of symbols. The method uses the gray scale information of captured images in order to reduce the complexity of execution.

The size of the gray scale image matrix Q, is m x n. It is then divided into equal size blocks of size w_1 x w_2 and the mean value of the data inside each block is calculated to form the dimensionality reduced representation. The newly formed mean value matrix is named as $\overline{Q}$ of size w_1 x w_2. The (i^{th}, j^{th}) element of $\overline{Q}$ or the mean value of each block in $\overline{Q}$ can be calculated by using the (18).

$$\overline{Q}(i, j) = \frac{1}{w_1 w_2} \sum_{x=\frac{m}{w_1}(i-1)+1}^{\frac{m}{w_1}i} \sum_{y=\frac{n}{w_2}(j-1)+1}^{\frac{n}{w_2}j} Q(x, y) \quad (18)$$

Breakpoints have to be applied to convert $\overline{Q}$ into a symbol matrix S or the 2D SAX representation. For this, a 'threshold' value is used so that breakpoints can be calculated easily. Threshold value is calculated using the (19).

$$T = \frac{\max - \min}{SAX_{level}} \quad (19)$$

Where 'max' is the maximum value in the $\overline{Q}$ matrix, 'min' is the minimum value in the $\overline{Q}$ matrix, and SAX_{level} is equal to number of symbols to be used.

For example, if four SAX_{level} are chosen, five breakpoints have to be calculated. The breakpoints are min, min+T, min+2T, min+3T and max. Then, one symbol is used to represent the values between min and min+T, and another symbol is used for the values between min+T and min+2T and so on. In this manner, the symbol matrix S, the 2D SAX representation can be obtained. Then, this two dimensional data is decomposed into one dimensional (1D) sequences using a progressive scan [4]. These 2D SAX representations as strings are stored in the database as palmprint template.

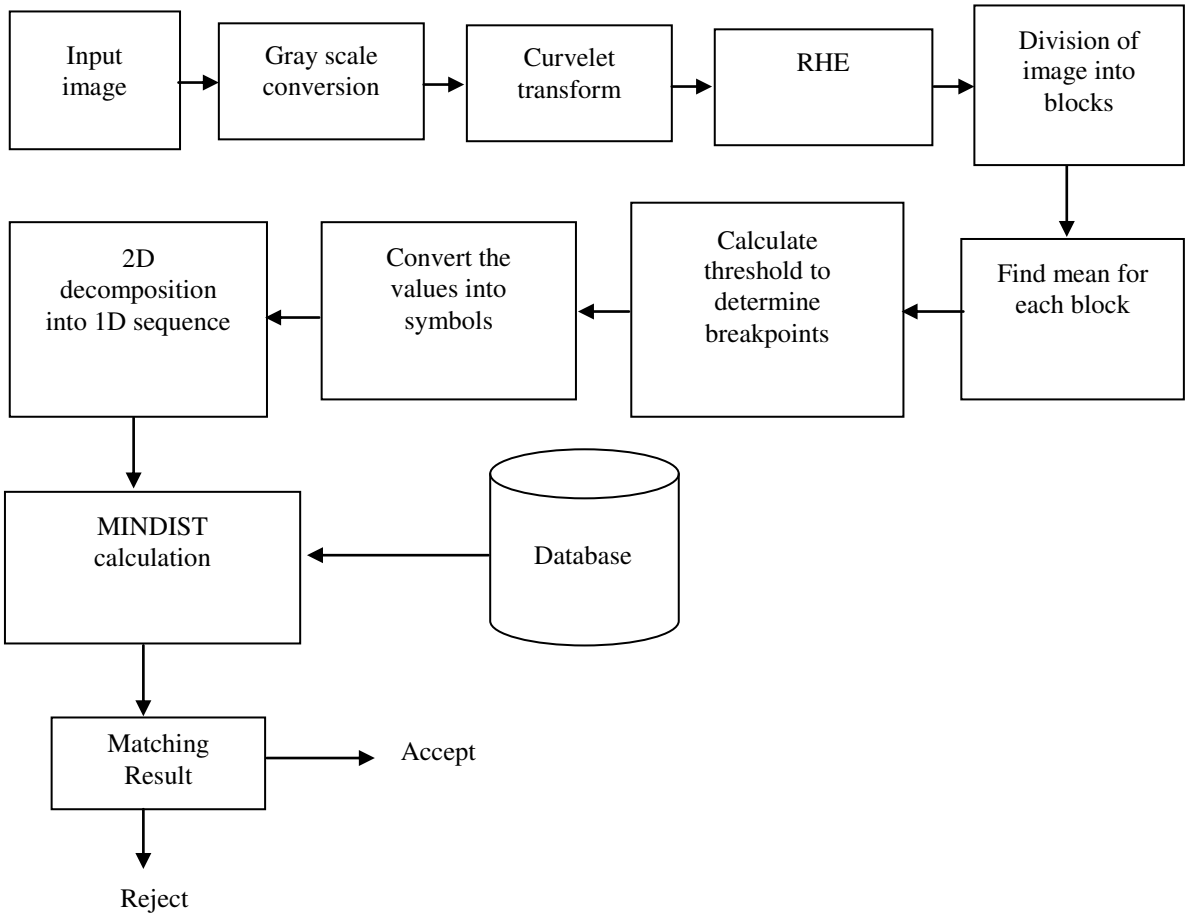

Figure-3. Block diagram of palmprint recognition using SAX features.

The MINDIST between two corresponding strings is measured and this is adopted as the similarity measurement of the corresponding two palmprints. Given two SAX strings $\hat{Q} = \hat{q}_{11}, \hat{q}_{12}, ...\hat{q}_{w_1 w_2}$ and $\hat{C} = \hat{c}_{11}, \hat{c}_{12}, ...\hat{c}_{w_1 w_2}$, their MINDIST can be calculated using the equation (20) where dist() can be implemented using lookup table as given in Table 3. If the MINDIST is smaller, then the two palmprints are more similar.

$$MINDIST(\hat{Q}, \hat{C}) = \sqrt{\frac{mn}{w_1 w_2}} \sqrt{\sum_{i=1}^{w_1} \sum_{j=1}^{w_2} dist(\hat{q}_{ij}, \hat{c}_{ij})^2} \quad (20)$$

where m x n is the size of the image and w_1 x w_2 is the SAX length. Few samples of palmprints are shown in Figure-3, in which palmprints in the same column are from the same palm, and the palmprints in the first and second rows are from session one and session two respectively.

Figure-4 shows the output of the palmprint enhancement and feature extraction process where block size (w1×w2) is set as 8×8 and the SAX_{level} as 4.

Table-3. Lookup table for calculating dist() function with four SAX_{level}

	A	**b**	**c**	**d**
a	0	0	0.67	1.34
b	0	0	0	0.67
c	0.67	0	0	0
d	1.34	0.67	0	0

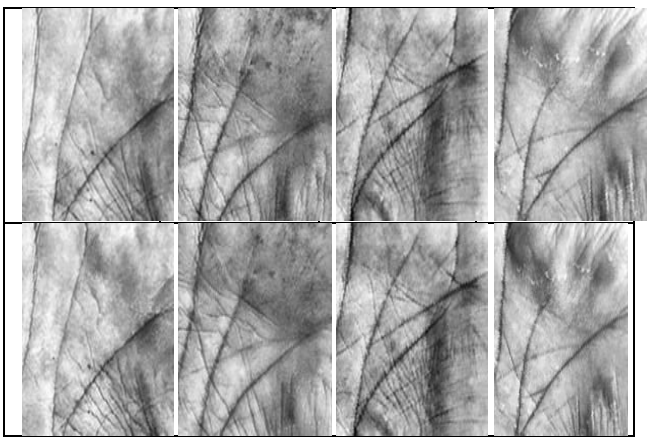

Figure-4. Sample palmprint.

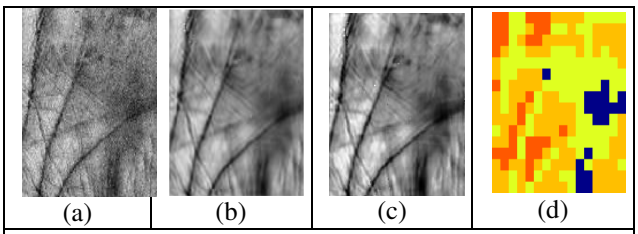

ddbbdddccccbbbbbddbbcddbbcbbccccddbcddcccccbccc
cdcbbcccbbbcbcbcccbbbbbbbbbbbbbbccbbcccabbbbbb
bbbdbccccbbbbbbbabbcbccdbccbbbaaabacbcdcbccccba
aaaacccdbccccccbbaabcbcdcbcccdcbbbbbcccdbdddccbb
bbbccdddbddcbccbabbcccdccdcbcccabcccbccbcdbccbb
aacccccccbcbccccbaacccc
(e)

Figure-5. Palmprint enhancement and feature extraction. (a) The input image, (b) Image after applying curvelet, (c) RHE equalized image, (d) SAX representation, (e) SAX string

The SAX string is used as palmprint templates for experiment-matching process. Figure-5 shows the four samples of a palmprint from an individual and their corresponding SAX representation.

SAX features are converted into numerical values and feature database is formed. For all the 234 subjects feature database is formed. In the present work in addition to the classification by minimum distance method, we also explored Support Vector Machine, Bayesian classifier and Random forest. An SVM classifies data by finding the best hyperplane that separates all data points of one class from those of the other class. The best hyperplane for an SVM means the one with the largest margin between the two classes. Margin means the maximal width of the slab parallel to the hyperplane that has no interior data points. Random forest operates by constructing a multitude of decision tree at training and outputting the class that is the mode of the classes (classification) or mean prediction (regression) of the individual trees. Naïve Bayes classifier assigns the class to the test input by calculating the posterior probability.

5. RESULTS AND DISCUSSIONS

234 subjects from IIT Database are used for recognition. Four samples are taken for each subject. The features of the palmprint image to be recognized are checked with the features of the palmprint images stored in the system's database.

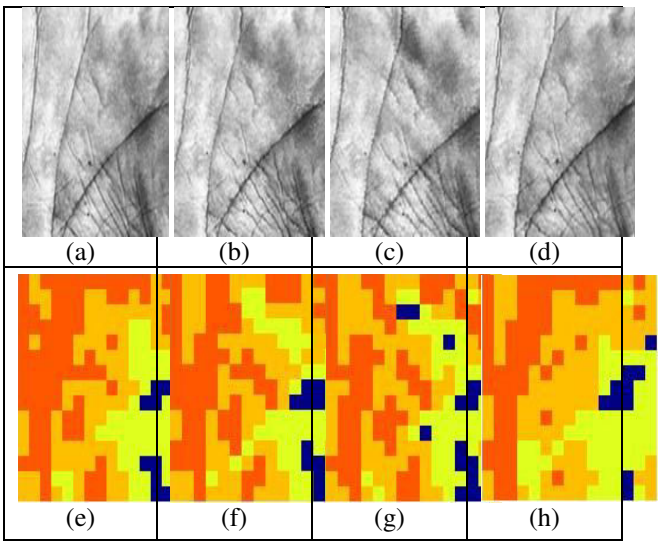

Figure-6. (a),(b),(c) and(d) palmprints from the same palm,(e),(f),(g) and (h) corresponding SAX representation.

If a match is found, then the person is authenticated, otherwise the person is unauthenticated. Verification is done with HE, curvelet, RHE and curvelet & RHE methods. It is proceeded with two phases in which in the first phase, 117 random palmprint images from the IIT database that are also contained in the system's database were tested. In the second phase, 117 palmprint images were taken for testing from the IIT database that is not in the system's database.

The performance of a palmprint authentication system can be measured by three metrics, namely FAR (False Acceptance Rate), FRR (False Rejection Rate) and TSR (Total Success Rate).

False Acceptance (FA) is the number of times the system accepts an unauthorized user (imposter) and FAR is the ratio of number of false acceptances to the total number of imposter accesses. FAR is measured as in (21).

$$FAR = \frac{\text{Number of false acceptances}}{\text{Total number of imposter accesses}} \times 100 \ \% \qquad (21)$$

False Rejection (FR) is the number of times the system rejects an authorized user (genuine) and FRR is the ratio of number of false rejections to the total number of genuine accesses. FRR is measured using (22).

$$FRR = \frac{\text{Number of false rejections}}{\text{Total number of genuine accesses}} \times 100 \ \% \qquad (22)$$

TSR (Connie *et al* 2005) represents the recognition rate of the system and it is measured using (23)

$$TSR = \left(1 - \frac{FA + FR}{\text{Total number of accesses}}\right) \times 100 \ \% \qquad (23)$$

5.1 Performance of Palmprint Recognition Using SAX Features

The comparison of FAR of the RHE & curvelet method with other methods is given in Figure-7. RHE & curvelet method has the lowest FAR. The comparison of FRR of the RHE & curvelet method with other methods is given in Figure-8. RHE & curvelet method has the least FRR.

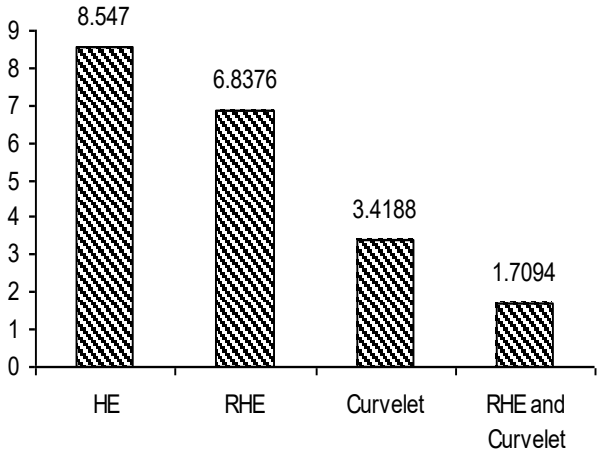

Figure-7. Comparison of FAR of RHE and curvelet method with HE, RHE and curvelet.

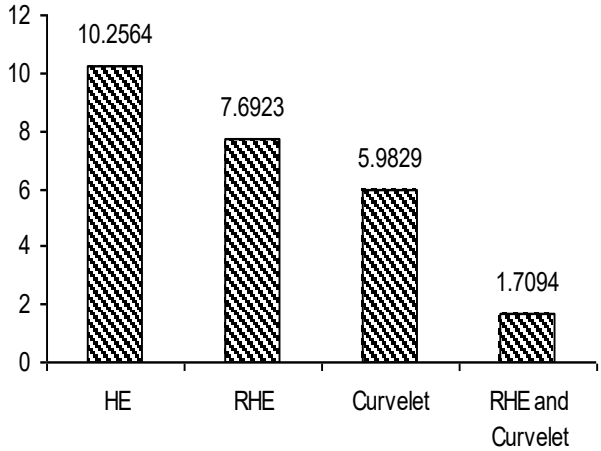

Figure-8. Comparison of FRR of RHE and curvelet method with HE, RHE and curvelet.

The comparison of TSR of the RHE & curvelet method with other methods is given in Figure-9. RHE & curvelet method has the highest TSR. Here, the proposed technique provides TSR of 98.29%.

The optimum result is obtained when both curvelet and RHE are used. The FAR, FRR and TSR values are measured as 1.7094%, 1.7094%, 98.2905%. Michael *et al* (2008) used contrast adjustment and smoothing as enhancement technique in contactless palmprint and recognition system. They obtained a recognition rate of 98.10 % without image enhancement and recognition rate of 98.68% with image enhancement. An improvement of 0.58 % is obtained using enhancement. The proposed system provides an improvement of 8% than the HE method using RHE and curvelet.

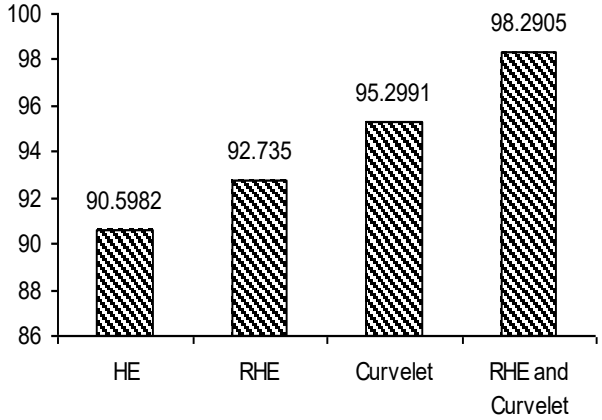

Figure-9. Comparison of TSR of RHE and curvelet method with HE, RHE and curvelet.

From Table-4 it is imperative with the combination of RHE & curvelet and SAX features; Random forest classifier gives the maximum total success rate. Table-4 it is imperative with the combination of RHE & curvelet and SAX features; Random forest classifier gives the maximum total success-rate.

Table-4. Analysis of the performance of the classifier.

Classifier used	Enhancement method	False Acceptance Rate/False Rejection Rate/Total Success Rate (%)
Minimum distance	RHE & Curvelet	1.7094/1.7094/98.2905
Support Vector Machine	RHE & Curvelet	1.253/1.53/98.3%
Bayesian Classifier	RHE & Curvelet	1.1/1.4/98.7
Random Forest classifier	RHE & Curvelet	0.9/1.1/99%

6. CONCLUSIONS

To improve the accuracy of palmprint authentication system, curvelet and RHE are applied prior to the 2D SAX conversion. As these procedures remove the noise and enhance the contrast, the proposed system ensures high performance with competitive accuracy. Since it is a texture-based approach, the computational complexity of the feature extraction process is much lower and thus can be efficiently implemented for even slow mobile embedded platforms. Also, the proposed approach does not rely on any parameter training process. Classification is done with minimum distance classifier, Support Vector Machine, Random Forest and Bayesian. Highest Total Success Rate is achieved in case of Random Forest classifier with minimum false acceptance and false rejection rate.

ACKNOWLEDGMENTS

The authors would like to thank Dr. Ajay Kumar of IIT, New Delhi for providing permission and help on downloading palmprint image database from IIT database.

REFERENCES

[1] Zhang David, Zhenhua Guo, Yazhuo Gong. 2016. An online system of multispectral palmprint verification. Multispectral Biometrics. Springer International Publishing. 117-137.

[2] Jaafar Haryati, Salwani Ibrahim, Dzati Athiar Ramli. 2015. A robust and fast computation touchless palm print recognition system using LHEAT and the IFkNCN classifier. Computational intelligence and neuroscience. (2015): 43.

[3] Zhang Lin, et al. 2017. Towards contactless palmprint recognition: A novel device, a new benchmark, and a collaborative representation based identification approach. Pattern Recognition. 69, 199-212.

[4] Zhang, Kunai, Da Huang, and David Zhang. 2017. An optimized palmprint recognition approach based on image sharpness. Pattern Recognition Letters, 85, 65-71.

[5] Li Gen and Jaihie Kim. 2017. Palmprint recognition with local micro-structure tetra pattern. Pattern Recognition. 61, 29-46.

[6] Raghavendra R. and Christoph Busch. 2015. Texture based features for robust palmprint recognition: a comparative study. EURASIP Journal on Information Security. 1(5).

[7] Huang, Da, Kunai Zhang, and David Zhang. 2015. Improvement on Gabor Texture Feature Based Biometric Analysis Using Image Blurring. International Conference on Intelligent Science and Big Data Engineering. Springer, Cham.

[8] Younesi Ali and Mehdi Chehel Amirani. 2017. Gabor Filter and Texture based Features for Palmprint Recognition. Procedia Computer Science. 108, 2488-2495.

[9] Nigam, Aditya, and Phalguni Gupta. 2014. Palmprint recognition using geometrical and statistical constraints. Proceedings of the Second International Conference on Soft Computing for Problem Solving (SocProS 2012), 28-30.

[10] Imtiaz, Hafiz and Shaikh Anowarul Fattah. 2013. A wavelet-based dominant feature extraction algorithm for palm-print recognition. Digital Signal Processing. 23.1, 244-258.

[11] Aykut, Murat and Murat Ekinci. 2015. Developing a contactless palmprint authentication system by introducing a novel ROI extraction method. Image and Vision Computing. 40, 65-74.

[12] Ekinci, Murat, and Murat Aykut. 2016. Kernel Fisher discriminant analysis of Gabor features for online palmprint verification. Turkish Journal of Electrical Engineering & Computer Sciences. 24(2). 10.1109/ICASSP.2004.1326597]

[13] Badrinath G. S., Gupta P. 2012. Palmprint based recognition system using phase-difference information. Future Generation Computer Systems. 28(1): 287-305 [doi: 10.1016/j.future.2010.11.029].

[14] Tamrakar D., Khanna P. 2016. Kernel discriminant analysis of Block-wise Gaussian Derivative Phase Pattern Histogram for palmprint recognition. J. Vis. Commun. Image Representation. [10.1016/j.jvcir.2016.07.008]

[15] Li H., Zhang Z. 2014. Research on palmprint identification method based on quantum algorithms. Scientific World Journal. [10.1155/2014/670328]

[16] Wang X., Huang S., Gao N., Zhang Z. 2014. 3D palmprint data fast acquisition and recognition. In Proc. of SPIE, 9279, 92790P-1.

[17] Palanikumar S., Minu Sajan., Sasikumar M. 2013. Advanced Palmprint recognition using unsharp masking and histogram equalization. IEEE International Conference on Information and

Communication Technologies. 47-52 [10.1109/CICT.2013.6558060].

[18] Palanikumar S., Sasi Kumar., Rajeesh J. 2013. Palmprint enhancement using recursive histogram equalisation. Imaging Science Journal. 61(5): 447-457 [doi:10.1179/1743131X12Y. 0000000031]

[19] Somvanshi Shivangi S. 2017. Comparative statistical analysis of the quality of image enhancement techniques. International Journal of Image and Data Fusion. 1-21. 10.1145/882082.882086].

[20] Lu G. M., Zhang D., Wang K. Q. 2003. Palmprint recognition using eignpalms features. Pattern Recogn. Lett., 24(9-10): 1463-1467, [10.1016/S0167-8655(02)00386-0]

[21] Shang L., Huang D. S., Du J. X. Zheng C. H. 2006. Palmprint recognition using FastICA algorithm and radial basis probabilistic neural network. Neurocomputing 69(13-15): 1782-1786, [10.1016/j.neucom.2005.11.004]

[22] Wu X., Zhang D., Wang K. 2003. Fisherpalms based palmprint recognition. Pattern Recogntion Letters. 24(15): 2829-2838. [10.1016/S0167-8655(03)00141-7]

[23] Badrinath G. S., Gupta P. 2011. Stockwell transform based palm-print recognition. Applied Soft Computing, 11(7): 4267-4281, [10.1016/j.asoc.2010.05.031]

[24] Xiao-Yuan Jing, David Zhang. 2004. A Face and Palmprint Recognition Approach Based on Discriminant DCT Feature Extraction. IEEE Transactions on systems and cybernetics-Part cybernetics, 34(6), [10.1109/TSMCB.2004.837586]

[25] Zhang, D. 2004. Palmprint Authentication, Norwell, Mass, Kluwer Academic Publishers.

[26] Kong, A., Zhang, D. and Kamel, M. 2006. Palmprint identification using feature level fusion. Pattern Recognition, 39(3): 478-487, [10.1016/j.patcog.2005.08.014]

[27] Adams Wai-Kin Kong, David Zhang. 2004. Competitive Coding Scheme for Palmprint Verification. International Conference on Pattern Recognition, pp. 520-523.[10.1109/ICPR.2004.257]

[28] Sun Z. N., Tan T. N., Wang Y. H. and Li S. Z. 2005. Ordinal palmprint representation for personal identification. Proceedings of IEEE International Conference on Computer Vision and Pattern Recognition, 1: 279-284, 2005.[10.1109/CVPR.2005.267]

[29] Gan J. Y. and Zhoul D. P. 2006. A novel method for palmprint recognition based on wavelet transforms. IEEE International Conference on Signal Processing, Vol.3, [10.1109/ICOSP.2006.345917]

[30] Meraoumia, Abdallah, Salim Chitroub, Ahmed Bouridane. 2014. Biometric recognition systems using multispectral imaging. Bio-inspiring Cyber Security and Cloud Services: Trends and Innovations. Springer Berlin Heidelberg. 321-347.